

A Biosynthetic Regulated Secretory Pathway in Constitutive Secretory Cells

Raymond A. Chavez,* Stephen G. Miller,† and Hsiao-Ping H. Moore*

*University of California at Berkeley, Department of Molecular & Cell Biology, Berkeley, California 94720-3200; and †Ligand Pharmaceuticals, San Diego, California

Abstract. It has frequently been proposed that while the constitutive secretory pathway is present in all cells, the regulated secretory pathway is found only in specialized cells such as neuronal, endocrine, or exocrine types. In this study we provide evidence that suggests that this distinction is not as restrictive as proposed. We have identified a population of post-Golgi storage vesicles in several constitutive secretory cells using [³⁵S]SO₄-labeled glycosaminoglycan (GAG) chains as a marker. A fraction of this pool of vesicles can undergo exocytosis in response to stimuli such as cytoplasmic Ca²⁺ and phorbol esters. The effect of Ca²⁺ was demonstrated both in intact cells in the presence of the ionophore A23187 and in streptolysin-O-permeabilized semi-intact cells. *N*-ethylmaleimide, under conditions known to block regulated and constitutive secretion, inhibited the stimulated secretion from these cells, sug-

gesting that the observed release of labeled GAG chains was not due to a leakage artefact. Subcellular fractionation revealed that the stored GAG chains were in low-density membrane granules ($d \sim 1.12$ g/ml), whose size was greater than that of synaptic-like vesicles found in PC12 cells. In addition, in CHO cells that express epitope-tagged rab 3D, the labeled GAG chains were found to cofractionate with the exogenous rab protein. When expressed in the regulated cell line AtT-20, this tagged rab protein was found to colocalize with ACTH-containing dense-core granules by indirect immunofluorescence. Taken together, these results provide evidence for the presence of a cryptic regulated secretory pathway in "constitutive" cells and suggest that the regulated secretory pathway is more widespread amongst different cell types than previously believed.

PROTEIN secretion from mammalian cells can be either constitutive or regulated. It has been generally assumed that while the constitutive pathway is ubiquitous in eukaryotic cells, the regulated pathway is not (for reviews see Burgess and Kelly, 1987; Miller and Moore, 1990). Several characteristics serve to distinguish these two pathways. The constitutive secretory pathway release of secretory products occurs at a consistent rate, reflective of an ongoing membrane flux to the cell surface. Constitutive vesicles do not accumulate to an appreciable degree. Regulated secretion, on the other hand, involves two distinct steps. Newly synthesized regulated secretory products are first stored within the cell, accumulated in vesicular structures. Upon stimulation, the contents of these regulated storage granules can undergo rapid release from the cell. In the absence of a secretory stimulus, the turnover of these granules is slow (basal release). The alteration of the intracellular levels of second messenger(s) is required to stimulate the release of the granule contents.

Studies using semi-intact cell systems have shown that the proximal signal for exocytotic release is a rise in free cytoplasmic Ca²⁺ ion (for review see Martin, 1994). In contrast, secretagogues do not appear to have a significant effect on traffic through the constitutive pathway. Neurons also possess an additional regulated pathway that originates from recycling endosomes rather than the biosynthetic path (for review see De Camilli, 1995). Regulated secretion is a hallmark of the endocrine, exocrine, and nervous systems, and cells containing a regulated secretory pathway are most often found in these tissues.

Emerging evidence suggests that many cells, including epithelial cells (for review see Matter and Mellman, 1994), liver cells (Saucan and Palade, 1994), and the budding yeast *S. cerevisiae* (Harsay and Bretscher, 1995), have more than one constitutive pathway. Cells outside the neural, endocrine, and exocrine systems have also been shown to possess synaptic-like regulated secretory pathway derived from endosomes. For example, adipocytes are able to transport the glucose transporter GLUT4 to the cell surface in response to insulin (Slot et al., 1991; Smith et al., 1991). The insertion and retrieval of other plasma membrane transporters, such as the gastric H⁺/K⁺-ATPase (Forte et al., 1989) and the renal water channel (Lencer et

Address all correspondence to H.-P.H. Moore, University of California at Berkeley, Department of Molecular & Cell Biology, 142 Life Sciences Addition #3200, Berkeley, CA 94720-3200. Tel.: (510) 643-6528. Fax: (510) 643-8708. e-mail: hpmoore@mendel.berkeley.edu

al., 1990), can be influenced by a variety of signals. Most recently, Steinhardt and coworkers have described the process of membrane resealing in sea urchin embryos and 3T3 fibroblasts that requires external calcium and is blocked by treatments that prevent synapse-like regulated secretion in other systems (Steinhardt et al., 1994). The shedding of cell surface transmembrane proteins, such as TGF α and APP (Sisodia, 1992; Bosenberg et al., 1993; Arribas and Massagué, 1995), occurs via a regulated process. In polarized epithelia, transcytosis and apical recycling can also be affected by phorbol esters (Cardone et al., 1994). These studies suggest that regulated membrane traffic may occur in the endocytic pathway in many cell types as a means to modify the composition of their plasma membranes rapidly. In contrast, regulated biosynthetic transport has only been demonstrated in endocrine, exocrine, or neuronal cells.

In the course of our studies on vesicular transport between the TGN and the cell surface, we have used glycosaminoglycan (GAG)¹ chains as a secretory marker. Using this approach, we have found a post-TGN storage pathway that shows similarities with the biosynthetic regulated secretory pathway in peptide hormone-secreting cells. We conclude that constitutive secretory cell lines contain a post-Golgi regulated secretory pathway, extending the presence of the regulated secretory pathway to a wide variety of cell types.

Materials and Methods

PCR and Molecular Biology Techniques

Total RNA from rat brain, CHO cells, rat pituitary, and AtT-20 cells was prepared as described (Sambrook et al., 1989). 5 μ g of the RNA were reverse-transcribed by standard methods using an oligo-dT primer and M-MuLV reverse-transcriptase (GIBCO BRL, Gaithersburg, MD). An aliquot from the reverse-transcription reaction was used as template for labeled PCR reactions. The reverse-transcription product was combined in a PCR reaction mixture spiked with α -[³²P]dCTP (3,000 Ci/mmol; Dupont-New England Nuclear, Boston, MA), and the reactions were cycled (25 cycles) as follows: 95°C, 30 s; 50°C, 2 min; 72°C, 3 min. A sample of each reaction was electrophoresed through a nondenaturing DNA acrylamide gel (Sambrook et al., 1989). The gel was dried and exposed to a PhosphorImager screen (Molecular Dynamics, Sunnyvale, CA). The PCR was used to clone rab 3C (mouse AtT-20 cells) and rab 3D (rat pituitary) from the reverse-transcription products using primers based on published sequences (Matsui et al., 1988; Baldini et al., 1992). The forward and reverse primers for each cloning PCR were designed with restriction sites for directional cloning of the resultant product into the vector pCDM8-FT (Chen et al., 1993), resulting in the creation of chimeras (pCDM8-FT-rab 3C and pCDM8-FT-rab 3D) composed of a short amino acid sequence derived from the influenza virus hemagglutinin (HA) protein (recognized by the mAb 12CA5; BAbCO, Berkeley, CA) at the amino-terminal end followed by the rab sequence. Sequences of the rab clones were determined by dideoxy sequencing with the Sequenase kit (US Biochemicals, Cleveland, OH). Sequence analysis was performed with the MacVector software package (IBI, New Haven, CT).

Cell Culture Conditions

AtT-20 F2 cells and PC12 cells were maintained as described (Chavez et al., 1994). CHO cells were maintained in Ham's F12 medium (BioWhittaker, Walkersville, MD) supplemented with 10% FBS at 37°C under 5%

CO₂. L cells were grown in DME containing 10% FBS at 37°C under 5% CO₂.

Stable Transfections

AtT-20 F2 and CHO cells were transfected by a modification of the calcium phosphate method previously described (Chavez et al., 1994) using a selectable marker plasmid (pSV2-*neo*; Southern and Berg, 1982) and either pCDM8-FT-rab 3C or pCDM8-FT-rab 3D. AtT-20 cells transfected with pCDM8-FT-rab 11 were provided by Dr. Y.-T. Chen (Stanford University, Stanford, CA). Stable clones from either transfection were screened by immunoblotting with mAb 12CA5.

Secretion of GAG Chains from Intact Cells

Constitutive secretion: AtT-20, L, and CHO cells grown in 12-well plates (1–5 \times 10⁵ cells per well) were rinsed with PBS, and then starved of sulfate in sulfate-free DME containing 1 mM 4-methylumbelliferyl- β -D-xyloside (xyloside; Sigma Chem. Co., St. Louis, MO) for 30 min. All incubations were carried out at 37°C. The cells were then radiolabeled with 150 μ Ci/ml [³⁵S]SO₄ (ICN Biochemicals, Costa Mesa, CA) for 2 h in the same medium. Cells from one well were extracted immediately after the labeling period to determine the amount of total label incorporated. Labeled cells in the parallel wells were chased in DME for three consecutive periods for 90 min (see Fig. 1 A). In a parallel experiment, 8-bromo cyclic AMP (8-Br cAMP; 5 mM final concentration) was added during the last 90 min of chase to stimulate secretion from regulated secretory granules (see Fig. 1 B). Media samples were collected after each chase and centrifuged in a microfuge for 10 min to remove cell debris. The remaining cells were extracted at the end of the last chase period using a Triton X-100 buffer. Both media and cell extract samples were processed for cetylpyridinium chloride (CPC) assays of GAG chains as described (Miller and Moore, 1992).

Regulated secretion: Cells grown in 12-well plates were labeled as described above except that the starvation and labeling medium was SBM (NaCl, 110 mM; MgCl₂, 10 mM; glucose, 5.55 mM; KCl, 5.4 mM; CaCl₂, 2 mM; Na₂HPO₄, 0.9 mM; Hepes, 20 mM, pH 7.2), the concentration of [³⁵S]SO₄ in the labeling reaction was 100 μ Ci/ml, and the labeling time was 30 min. The cells were chased for two 60-min periods with DME containing 5 mM Na₂SO₄ to allow constitutive secretion to occur. To trigger secretion from storage pools, the cells were incubated for 15–30 min at 37°C in 0.5 ml of either DME alone, DME (1.8 mM CaCl₂) plus 1 μ M A23187, SBM containing 2 mM EGTA and 1 μ M A23187, or DME containing 50 ng/ml phorbol 12-myristate 13-acetate (TPA; see Fig. 2). All chase and stimulation media contained 5 mM Na₂SO₄. Radiolabeled GAG chains released into the medium and remaining in the cell extracts were determined using the CPC precipitation assay.

GAG Chain Secretion from Semi-intact Cells

L and CHO cells grown in 12-well plates were incubated with 0.5 mM xyloside in SBM for 30 min at 37°C to initiate GAG chain formation, and then labeled with 100 μ Ci/ml [³⁵S]SO₄ in SBM and 0.5 mM xyloside for 2 h at 37°C. The cells were chased for two consecutive 90-min periods in DME containing 5 mM Na₂SO₄. Cells were then permeabilized with streptolysin-O (SL-O; Burroughs-Wellcome, Research Triangle Park, NC) as described previously (Miller and Moore, 1991, 1992). The total Ca²⁺ concentration in transport buffer was adjusted to give the indicated concentration of free Ca²⁺ (see Figs. 3 and 4). Incubation of semi-intact cells was carried out at 37°C for 30 min. A parallel sample was sham-permeabilized and incubated in SBM for 4 min at 37°C, followed by the incubation in SBM for 30 min at 37°C. Labeled GAG chains either released into the medium or extracted from the remaining cells were assayed by the CPC precipitation procedure. In some cases, cells that had been labeled and chased were treated with *N*-ethyl maleimide (NEM; 0.2 mM) on ice for 15 min and quenched with DTT before SL-O treatment (see Fig. 4 A).

Glycerol Velocity Gradient

To compare the relative sizes of GAG-containing granules from CHO cells and from synaptic vesicles from PC12 cells, homogenates of PC12 cells and [³⁵S]sulfate-labeled CHO cells were separated on glycerol velocity gradients (Herman et al., 1994). CHO cells were labeled as described (Regulated secretion, above). At the end of the chase period, the medium was discarded, and the cells were rinsed with buffer B (NaCl, 150 mM; EGTA, 1 mM; MgCl₂, 0.1 mM; Hepes, 10 mM, pH 7.4). Labeled cells were

lifted from the dish, washed, and resuspended in buffer B with PMSF (0.5 mM). The cells were homogenized by passage through an EMBL homogenizer (European Molecular Biology Laboratory, Heidelberg, FRG) and centrifuged at 9,000 rpm (9,680 g) in an SS-34 rotor (Sorvall Instrs., Wilmington, DE) for 4 min at 4°C to prepare a postnuclear supernatant fraction (S1). 400 µl of the S1 was loaded onto a 5–25% (vol/vol) glycerol/buffer B linear gradient. The gradients were spun in a 50.1 Ti rotor for 1 h at 4°C at 25,000 rpm; at higher speeds the GAG chains were found in the bottom third of the gradient (Chavez, R.A., and H.-P.H. Moore, data not shown). Fourteen gradient fractions (~350 µl) were collected. Membranes from these fractions were pelleted as described above and assayed for labeled GAG chains by the CPC precipitation assay after first solubilizing an aliquot of the pellets with 1% Triton X-100. The remainder of the gradient fraction was dried and resuspended in SDS sample buffer and an aliquot was analyzed by SDS-PAGE and immunoblotting (see below).

For PC12 cells, an S2 supernate enriched in synaptic-like vesicles (Linstedt and Kelly, 1991) was loaded onto the gradient. The S2 was prepared by further centrifugation of the S1 supernate (see above) at 16,000 rpm (30,600 g) in an SS-34 rotor for 35 min at 4°C. After fractionation on the glycerol velocity gradient, the individual fractions were pelleted and analyzed for the presence of synaptophysin, a synaptic vesicle protein, by immunoblotting (see below). The peak of synaptophysin immunoreactivity corresponded precisely with that described previously for this gradient system (Herman et al., 1994); (Chavez, R.A., and H.-P.H. Moore, data not shown).

D₂O-Sucrose Gradient

CHO cells pulse-labeled with [³⁵S]sulfate as described above (see Regulated secretion) were homogenized by repeated passage through a 23-g needle and the homogenate was centrifuged for 10 min at 1,000 g. The postnuclear supernate was loaded onto a 100% D₂O/10–50% sucrose step gradient as described in Miller et al. (1992). For Fig. 10 C, the gradient solutions contained 50% D₂O. 1-ml fractions were collected from the top. The membranes in these fractions were pelleted by diluting the fraction with cold PBS, and centrifuging for 30–40 min in a tabletop ultracentrifuge (TL-100; Beckman Instrs., Fullerton, CA) at 100,000 g at 4°C.

Electrophoresis and Immunoblotting

Laemmli sample buffer containing 5% β-mercaptoethanol was added to each aliquot of pelleted gradient fractions and the samples were subjected to SDS-PAGE (12.5%). After electrophoresis, the gels were electrotransferred onto Hybond nitrocellulose (Amersham Corp., Arlington Heights, IL). The immunodecoration pattern was revealed by the Amersham enhanced chemiluminescence method, following the manufacturer's protocol. The primary antibodies used were 12CA5 (anti-HA epitope tag; BAbCO); anti-rab 3 (Cl 42.1; Dr. R. Jahn, Yale University); and SY38 (anti-synaptophysin; Boehringer Mannheim Biochemicals, Indianapolis, IN). Data were recorded by exposure to Hyperfilm βMax (Amersham). In some cases blots were reprobed after treatment with stripping buffer (100 mM β-mercaptoethanol, 2% SDS, 62.5 mM Tris-HCl, pH 6.7) at 50°C for 30 min (see Fig. 6).

Immunofluorescence and Related Procedures

AtT-20 F2 cells, transfected and wild-type, were prepared for indirect immunofluorescence as previously described (Miller and Moore, 1991). The cells were seeded onto glass coverslips treated with mouse laminin (GIBCO BRL). The secondary antibody (fluorescein- or rhodamine-conjugated) was obtained from Organon-Teknika (Durham, NC).

The distribution of FT-rab 3D in CHO-FT-rab 3D cells was also performed by indirect immunofluorescence. The FT-rab 3D staining pattern was compared to that of hamster transferrin receptor using mAb H68.4 (White et al., 1992) (Zymed Laboratories, South San Francisco, CA) and the ER resident protein calnexin using an anti-calnexin pAb (Stressgen Biotechnologies Corp., Victoria, BC, Canada). In addition transient transfection was used to express the rat glucose transporter GLUT4 (a generous gift of Drs. F. Bonzelius and R. Kelly, University of California, San Francisco, CA) and a TGN38 chimera in CHO-FT-rab 3D cells by using the Lipofectamine reagent (GIBCO BRL) following the manufacturer's instructions. The distribution of GLUT4 in transfected cells was revealed with a polyclonal Ab raised against rat GLUT4 (James et al., 1989) (East Acres Biologicals, Southbridge, MA), using an alternate permeabilization protocol (Herman et al., 1994). Epitope-tagged TGN38 (TGN38-Ig) was a gift of K. Teter (University of California, Berkeley, CA) and was con-

structed by fusing the transmembrane and cytoplasmic domains of TGN38 (Luzio et al., 1990) to the carboxy-terminal side of the human IgG constant region; in transfected CHO cells, the tagged protein was found to colocalize with the TGN marker, furin (Lin, S., and H.-P.H. Moore, unpublished observation).

Photomicrographs were taken through a Zeiss Axiophot fluorescence microscope (Carl Zeiss, Thornwood, NY). Some specimens were analyzed with a Zeiss LSM Laser Scan Microscope with a z-interval of 300 nm using a 63× objective (see Fig. 8).

Results

Presence of a Post-Golgi Storage Site for Sulfated GAG Chains in Regulated and Constitutive Secretory Cells

This study originated from preliminary observations that we made during the course of developing a generalized quantitative method to measure TGN-to-cell surface transport in a variety of cell types. The method is based on the generation of a fluid-phase tracer, GAG chains, in the Golgi by treating cells with a membrane-permeant xyloside derivative (Miller and Moore, 1992). These chains can be labeled with [³⁵S]SO₄ in the *trans*-Golgi and/or TGN, providing a useful marker for pulse-chase analysis of vesicular traffic between the TGN and the cell surface. Analysis of AtT-20 cells, a tumor cell line derived from corticotrophes in the mouse anterior pituitary, has shown that [³⁵S]SO₄-labeled GAG chains exiting the TGN enter both the constitutive and the regulated secretory pathways (Brion et al., 1992). When incubated with xyloside and [³⁵S]SO₄, AtT-20 cells synthesized sulfated chondroitin sulfate GAG chains that migrated on SDS gels as a radiolabeled ladder centered ~14 kD (Burgess and Kelly, 1984; Brion et al., 1992). The labeled chains can be quantitated by a simple CPC precipitation/filtration assay (Miller and Moore, 1992).

A typical pulse-chase secretion assay with labeled GAG chains is shown in Fig. 1. AtT-20 cells incubated in xyloside and [³⁵S]SO₄ for 2 h export a fraction of the labeled GAG chains rapidly. 56% of total labeled chains were secreted within the first 90 min of chase; very little was secreted with additional chase time (<10% between 90 min and 270 min of chase, Fig. 1, *open bars*). After 270 min, 33% of labeled GAG chains were retained in the cells. Since constitutive secretion from the TGN occurs with a *t*_{1/2} of 20 min and secretion via the regulated secretory pathway exhibits a much longer half-time (~10 h in unstimulated cells; Moore and Kelly, 1985), these data suggest that 67% of the cellular GAG chains produced during the 2-h labeling period were exported constitutively. As we have shown previously, the remainder of the labeled GAG chains in AtT-20 cells were packaged into dense-core granules (Moore et al., 1983b). This can be demonstrated by stimulating the cells with a secretagogue during the plateau phase. As shown in Fig. 1 B, addition of 8-Br cAMP to labeled AtT-20 cells after 180 min of chase stimulated secretion of labeled GAG chains from the storage pool; ~40% of the labeled GAG chains remaining after the 180-min chase was released during a 90-min incubation with the secretagogue compared to 8% from unstimulated cells. This extent of stimulated release is similar to that previously observed for peptide hormones; 5 mM 8-Br cAMP induces the secretion of ACTH from dense-core

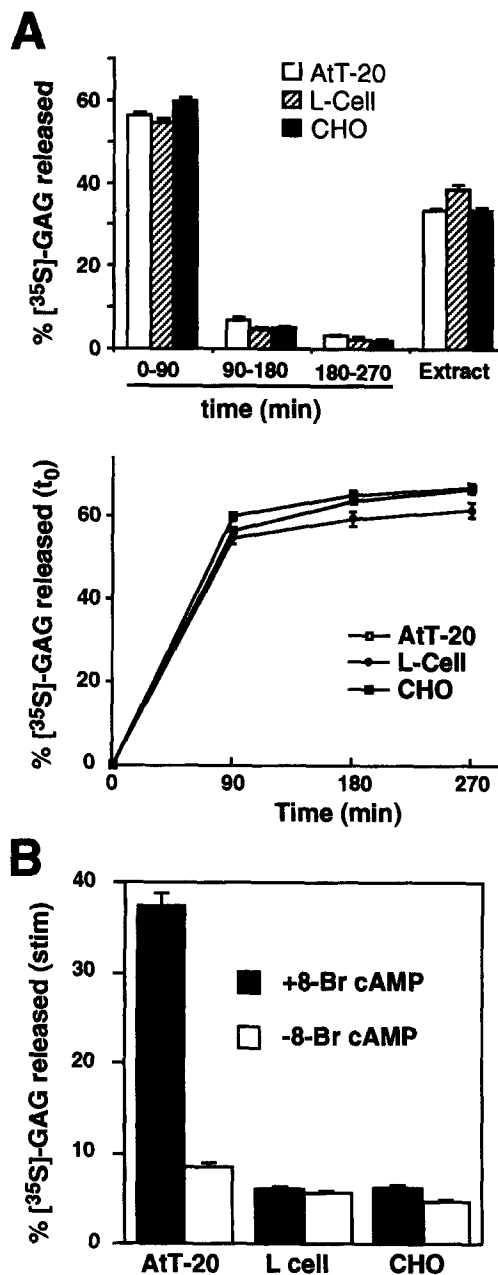
granules at a rate of ~20% per hour (linear up to at least 3 h). Thus, these data support the previous conclusion from subcellular fractionation studies (Moore et al., 1983b; Burgess and Kelly, 1984) that a substantial fraction of the stored GAG chains in AtT-20 cells reside within regulated peptide hormone-containing secretory granules.

Previous secretion studies have suggested that cell types such as L cells or CHO cells are strictly constitutive; in these cells, transfected growth hormone and proinsulin are rapidly secreted without storage (Moore et al., 1983a; Kreiner and Moore, 1990). Therefore, GAG chains labeled in the TGN are expected to exit these cells with the simple kinetics characteristic of the constitutive pathway. Indeed, we have shown that GAG chain synthesis can be induced in CHO cells and that after a short pulse-labeling period (2–5 min) the majority of the GAG chains are exported constitutively with a half-time of 20 min (Miller and Moore, 1991). Under the 2-h labeling conditions described here, we also found that a fraction of the labeled GAG chains is secreted with a $t_{1/2}$ of 20 min (Fig. 1; data not shown). However, we noticed that not all labeled GAG chains were released with such rapid kinetics. Instead, a fraction of the labeled GAG chains remained within the cells even after extensive chases. This is especially noticeable when the labeling period was extended (30 min–2 h). Fig. 1 A compares the kinetics of GAG chain secretion from L and CHO cells, two cell types whose secretion characteristics are considered to be solely constitutive, to those from the regulated secretory cell line, AtT-20, using identical labeling conditions. We were surprised to find that all three cell types showed a very similar extent of constitutive secretion: ~55–60% of the GAG chains labeled during a 2-h period were released within the first 90 min chase, with little further secretion during the ensuing 3 h. In all three cell types, 30–40% of the total label remained associated with the cells even after a 4.5-h chase. The calculated $t_{1/2}$ of GAG chain secretion during the plateau phase was >10 h (data not shown). SDS-PAGE analysis of media and extract samples confirmed that sulfated GAG chains with an average molecular size of 14 kD were synthesized and secreted from both cell types (Miller et al., 1992; data not shown).

Regulated Secretion of Stored GAG Chains from CHO and L Cells

The fraction of GAG chains that remained associated with CHO and L cells after extensive chases could arise from several possible sources. First, GAG chains are constitutively secreted from the TGN, but a fraction of the labeled chains may be re-endocytosed from the incubation medium and directed to either endosomes or lysosomes. Sec-

Figure 1. Comparison of GAG chain secretion from a “regulated” secretory cell type (AtT-20) and two “constitutive” secretory cell types (L cells and CHO cells). AtT-20, L, and CHO cells were labeled as described in Materials and Methods. The labeled cells were chased in DME for three 90-min periods. The labeled GAG chains recovered in the chase media and remaining in the cells after chase were assayed by the CPC precipitation method. The GAG-associated radioactivity from each chase medium and



cell extract was normalized to the total GAG-associated cpm recovered from an identical well of cells extracted immediately after the labeling period. (A, upper panel) Release of labeled GAG chains during each chase interval. Values represent percentages of GAG chain release during the indicated intervals and remaining in the cells at the end of the chase (Extract), relative to total sulfate incorporation into GAG chains. (A, lower panel) Time course of secretion of labeled GAG chains. Values represent cumulative percentages of GAG chain release at the end of each interval, relative to total sulfate incorporation into GAG chains at chase time 0 min. Data represent the average \pm SEM of triplicate determinations. (B) Release of labeled GAG chains in response to 8-Br cAMP. Cells were labeled as described and chased for two 90-min periods. The cells were then incubated in chase medium in the presence or absence of 5 mM 8-Br cAMP for a 90-min stimulation period at 37°C. Values shown are the amount of labeled GAG chains released during the stimulation period relative to the amount remaining in the cells at the start of the stimulation period, and represent the average \pm SEM of triplicate determinations.

ond, a fraction of the GAG chains may be incorporated into transport vesicles containing mannose-6-phosphate receptors and are delivered directly from the TGN to late endosomes/lysosomes. Third, there may be a post-Golgi storage compartment in these cells that is analogous to the dense-core secretory granules found in cells that possess a well-defined regulated pathway. This compartment would be in communication with the TGN; therefore a fraction of the labeled GAG chains becomes incorporated into this compartment. The first possibility was ruled out by a cross-feeding experiment. GAG chains that were constitutively secreted from labeled CHO cells into the medium during the first chase (Fig. 1) were collected, incubated with an equal number of unlabeled cells for 3 h at 37°C, and the amount of GAG chains associated with the cells was then determined by the CPC assay. Cells fed with labeled GAG chains took up <3% of the total label in the medium (data not shown); this amount is 20-fold lower than the observed cell-associated GAG chain storage pool (Fig. 1, Extract, is 62% of the amount in the 0–90-min medium). Thus, the cell-associated GAG chains did not arise from re-uptake of secreted material.

To distinguish between the second and third possibilities, we sought to determine if the stored GAG chains could be released by stimulation with a secretagogue. Cells were labeled and chased extensively to chase away labeled GAG chains in the constitutive pathway. The ability of 8-Br cAMP to stimulate secretion from the remaining pool of cell-associated [³⁵S]GAG chains was then examined. As shown in Fig. 1 B, incubation of labeled and chased CHO cells or L cells with 5 mM 8-Br cAMP for 90 min at 37°C did not result in the enhanced release of GAG chains; similar treatment of AtT-20 cells induced secretion approximately fivefold. However, GAG chain release from CHO or L cells could be induced in a calcium-dependent manner by the addition of 1 μM A23187 to the incubation medium (Fig. 2, columns 1 and 2); the addition of A23187 in the absence of extracellular Ca²⁺ did not stimulate GAG chain secretion (Fig. 2, column 3). The level of release from CHO cells was similar to that seen in ionophore-treated AtT-20 cells, which was 32% of the GAG chains remaining in the cells at the start of the stimulation period (data not shown), and similar to that seen in SL-O permeabilized AtT-20 cells labeled under the same conditions (Miller and Moore, 1991). We also tested the effects of phorbol esters on secretion, since these agents often trigger regulated exocytosis from storage granules. As shown in Fig. 2 (columns 4), TPA at a concentration of 50 ng/ml also enhanced the secretion of GAG chains from the storage pool. The effect of TPA on GAG chain secretion was more pronounced on L cells than on CHO cells. These results suggest that the stored GAG chains reside in compartments capable of regulated exocytosis. In pituitary corticotrophs, cAMP-dependent protein kinase activates calcium channels to trigger ACTH secretion (Luini et al., 1985). The lack of stimulation of secretion by cAMP in CHO and L cells is due to the absence of cAMP-activatable calcium channels in these cells (Sculptoreanu et al., 1993).

The regulated secretion we have observed is not the result of the shedding of cell surface-associated proteoglycans. SDS-PAGE analysis of media samples and cell ex-

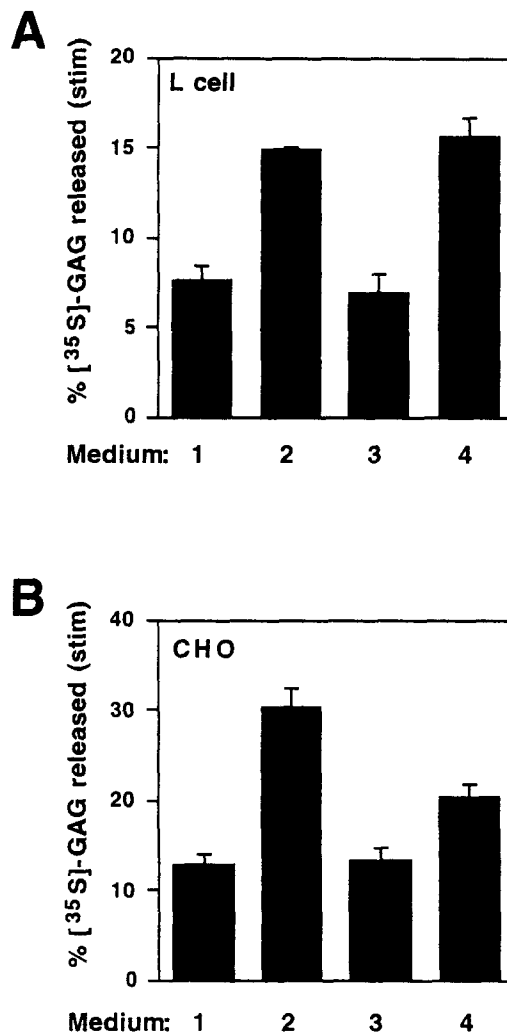


Figure 2. Stimulated release of GAG chains from intact AtT-20, L, and CHO cells in response to Ca²⁺ ionophore and the phorbol ester TPA. L and CHO cells were labeled as described in Materials and Methods. Labeled GAG chains in the constitutive pathway were then chased by two 60-min incubations in DME. The labeled cells were then incubated in various media for a 15-min stimulation period at 37°C: medium 1, DME containing 1.8 mM CaCl₂; medium 2, DME containing 1.8 mM CaCl₂ plus 1 μM A23187; medium 3, SBM containing 2 mM EGTA plus 1 μM A23187; and medium 4, DME containing 1.8 mM CaCl₂ plus 50 ng/ml TPA. Radiolabeled GAG chains released into the medium and those remaining in the cells were determined using the CPC precipitation assay. (A) Secretion from L cells and (B) secretion from CHO cells. Values shown are the amount of labeled GAG chains released during the stimulation period relative to the amount remaining in the cells at the start of the stimulation period, and represent the average of duplicate determinations; the range of values is also indicated.

tracts showed that the material secreted by labeled CHO cells under stimulated conditions and detected in our CPC assays was indeed free GAG chains; no high molecular weight proteoglycans were detected either in the media or in the cells (data not shown).

To examine further the secretion characteristics of this storage pool, we turned to a semi-intact cell system in which the cytoplasmic conditions can be more precisely

controlled. Previously we have shown that both constitutive and regulated secretion can be reconstituted in cells perforated with the bacterial agent streptolysin-O (SL-O) by supplying an ATP-regenerating system and cytosol (Miller and Moore, 1991, 1992; Carnell and Moore, 1994). In this system, the rate of constitutive secretion is independent of cytoplasmic calcium levels while regulated secretion is enhanced by micromolar calcium. Labeled and chased CHO or L cells were treated with SL-O and incubated in transport buffers containing various concentrations of buffered free calcium (Miller and Moore, 1992). As shown in Fig. 3, semi-intact cells incubated in low calcium (<10 nM free) released similar amounts of labeled GAG chains compared to unpermeabilized control cells. Raising the cytoplasmic free calcium concentration to 1 μ M with an EGTA/Ca²⁺ buffer enhanced secretion from the storage pool by about fourfold. The dose-response curve of calcium concentration showed maximal stimulation in the range of 1–10 μ M (data not shown), which is similar to those reported for regulated exocytosis of dense-core granules from AtT-20 or PC-12 cells (Ahnert-Hilger et al., 1985; Miller and Moore, 1991; Carnell and Moore, 1994).

Recent studies have shown that most heterotypic fusion events between compartments require the function of a NEM-sensitive factor, NSF (Block et al., 1988; Rothman, 1994). We therefore tested the effects of NEM on the observed GAG chain secretion. As shown in Fig. 4 A, pretreatment of semi-intact CHO cells with low concentrations of NEM (0.2 mM) on ice for 15 min (conditions that inactivate NSF) abolished the calcium-induced secretion of the stored GAG chains.

Furthermore, the observed calcium-induced release is not dependent on the addition of exogenous cytosol; inclusion of a 60-min wash out period before stimulation did not reduce the level of calcium-induced secretion (Fig. 4 B). We have previously observed that constitutive secretion in this system is sensitive to cytosol washout, most probably reflecting the requirement for small diffusible factors. In contrast, regulated secretion from SL-O-permeabilized PC12 cells is relatively insensitive to cytosol wash-out (Miller and Moore, 1991; Carnell and Moore, 1994). Taken together, the “regulated” exocytosis of GAG chains in CHO and L cells exhibits similar characteristics as the bona fide regulated exocytic pathway.

Expression of rab 3 Isoforms in CHO and AtT-20 Cells

One of the hallmarks of all forms of regulated secretion, both recycling (i.e., synaptic vesicle) and biosynthetic (i.e., dense-core granule) modes, is the presence of one or more members of the rab 3 subfamily of small GTP-binding proteins (Fischer von Mollard et al., 1994). These rabs appear to be associated exclusively with membranes involved in regulated secretion. Rabs 3A-C have been detected in neuronal tissues and cell types with well-defined regulated secretory pathways (Matsui et al., 1988; Oberhauser et al., 1994; Baldini et al., 1995) while rab 3D has a more widespread distribution (Baldini et al., 1992). We set out to determine if members of the rab 3 subfamily were present in AtT-20 and CHO cells. Total RNA was reverse-transcribed from rat brain, AtT-20 cells, and CHO cells using a poly(dT) primer, and the resulting cDNAs were used as

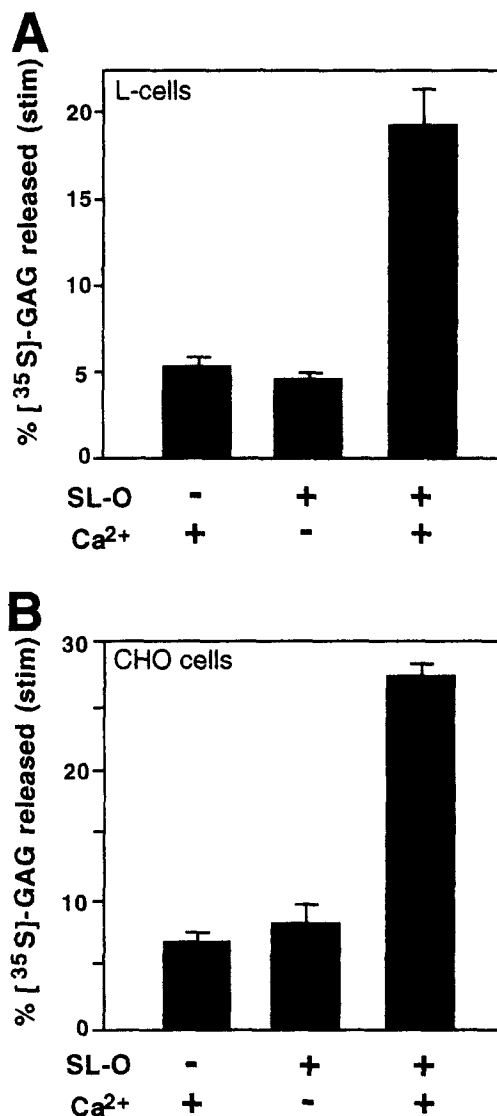


Figure 3. Ca²⁺-stimulated release of GAG chains from SL-O-permeabilized CHO and L cells. CHO and L cells were labeled as described in Materials and Methods. The cells were chased for two consecutive 90-min periods in unlabeled medium. The labeled cells were then permeabilized with SL-O as described, and incubated in transport buffer containing an ATP-regenerating system and cytosol at 37°C for a 30-min stimulation period. The free Ca²⁺ concentration in the transport buffer was adjusted to either 1 μ M (Ca²⁺: +) or <10 nM with EGTA (Ca²⁺: -). Control cells were sham-permeabilized in a buffer lacking SL-O (SL-O: -), and incubated in SBM for 30 min. Values shown are the amount of labeled GAG chains released during the stimulation period relative to the amount remaining in the cells at the start of the stimulation period. (A) Secretion from semi-intact L-cells; and (B) secretion from semi-intact CHO cells. Values represent the average + SEM of triplicate determinations.

templates for PCR amplification. Rat brain RNA was included as a positive control. Using the PCR and primers specific for the different rab 3 species identified so far, we have detected the expression of three members of the rab 3 subfamily in AtT-20 cells: rabs 3A and 3C (data not shown), and rab 3D (Fig. 5). In contrast, we were unable to detect rab 3A or rab 3C messages in CHO cells (data

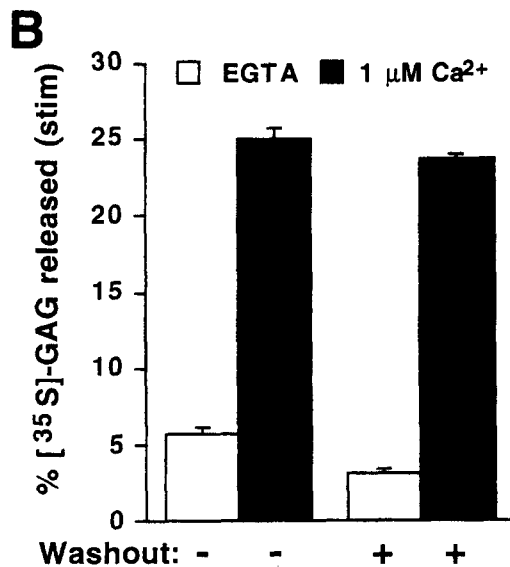
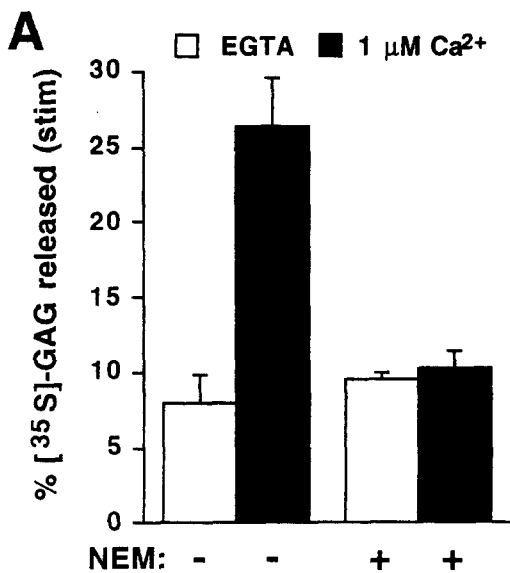


Figure 4. NEM sensitivity and cytosol independence of calcium-dependent release of GAG chains from semi-intact CHO cells. (A) Sensitivity to NEM. CHO cells were labeled and chased as described (see Fig. 3). Cells were treated with or without 0.2 mM NEM on ice for 15 min, rinsed, and incubated in DME containing 1 mM DTT on ice for 15 min to quench residual NEM. The cells were then permeabilized and secretion assayed by incubating the cells for a 15-min stimulation period at 37°C as described. For the unstimulated condition the free [Ca²⁺] in the transport buffer was adjusted to <10 nM, whereas for the stimulated condition the transport reaction contained 1 μM buffered free Ca²⁺. Open columns represent secretion under low-Ca²⁺ conditions (designated as “EGTA”), and filled columns represent secretion under high-Ca²⁺ conditions (designated as “1 μM Ca²⁺”). (B) Insensitivity to cytosol wash-out. CHO cells were labeled and chased as in A. After SL-O permeabilization, some cells were immediately cooled to 0°C and incubated in transport buffer including 5 mM EGTA for 60 min to allow the cytosol to leak out (washout: +). The cells were then warmed up to 37°C and incubated in transport buffer containing <10 nM free Ca²⁺ (open columns) or 1 μM free Ca²⁺ (filled columns) for a 15-min stimulation period. Parallel wells that had not been chilled were incubated immediately after SL-O

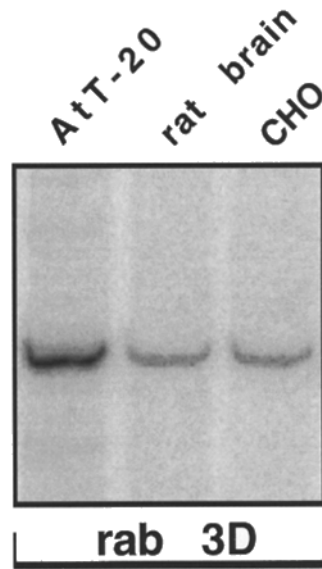


Figure 5. PCR analysis of rab 3D in AtT-20 cells, rat brain, and CHO cells. Five micrograms of total RNA from AtT-20 cells, rat brain, and CHO cells were reverse-transcribed using an oligo-(dT) primer. An aliquot of the resulting cDNA was used as template in polymerase chain reactions containing α-[³²P]dCTP with primers specific for rab 3D. Aliquots of each PCR were resolved on a urea-acrylamide gel, and analyzed with a PhosphorImager (Molecular Dynamics).

not shown). We therefore limited our focus to rab 3D. Fig. 5 shows a PCR analysis of the expression of rab 3D in rat brain and AtT-20 and CHO cells. Rab 3D was detected in AtT-20 cells and rat brain as well as in CHO cells. The identities of these amplification products were further confirmed by sequence analysis (see below). While we cannot exclude the presence of additional rab 3 isoforms in CHO cells, these data are consistent with the reported distributions of rab 3D in mammalian tissues. The presence of rab 3 family members in constitutive cells like the CHO cell line suggests that a regulated release mechanism may exist in these cells.

Stable Transfection of Epitope-tagged rab 3 Isoforms

To test if the rab 3 isoforms are indeed associated with membrane compartments involved in regulated exocytosis, we sought to analyze the subcellular localization of rab 3 in AtT-20 and CHO cells. We first used the antibody mAb Cl42.1 (Matteoli et al., 1991), which recognizes all isoforms of rab 3, to detect expression of endogenous rab 3 proteins by Western immunoblot analyses. In wild-type AtT-20 cells, a species of the correct electrophoretic mobility was recognized by this mAb, indicating that these cells indeed express rab 3 proteins (Fig. 6, upper left panel, lane wt). However, because all rab 3 isoforms are recognized by Cl42.1 (see below) and exhibit very similar electrophoretic mobilities, we were unable to distinguish the rab 3 isoforms by this method. Western blot analysis of wild-type CHO cells with Cl42.1 did not reveal detectable levels of rab 3 crossreactivity (Fig. 6, lower left panel, lane wt), presumably due to the relatively low expression of rab 3D in CHO cells compared to total rab 3 proteins in AtT-20 cells.

permeabilization with the appropriate stimulation medium (washout: -). Values shown are the amount of labeled GAG chains released during the stimulation period relative to the amount remaining in the cells at the start of the stimulation period. Values represent the average + SEM of triplicate determinations.

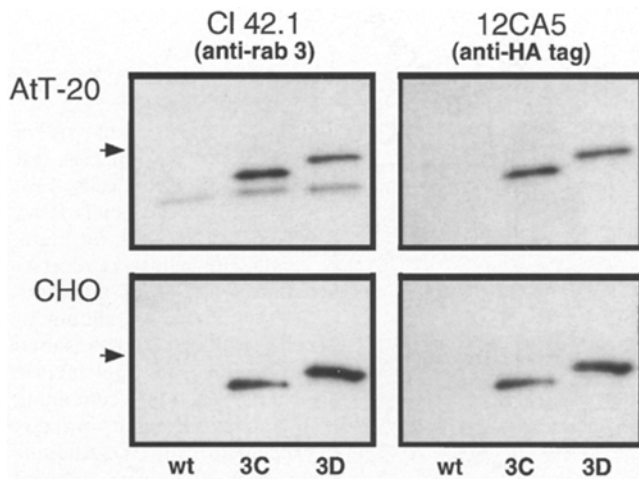


Figure 6. Immunoblot analysis of wild-type and stably transfected CHO and AtT-20 cells. Cell lysates ($\sim 10 \mu\text{g}$ protein/lane) from AtT-20 and CHO cells were resolved by SDS-PAGE (12.5%), transferred onto a nitrocellulose membrane, and immunoblotted with either an HA epitope-specific mAb (12CA5) or a rab 3-specific mAb (Cl 42.1), followed by HRP-conjugated anti-mouse secondary antibody. For both CHO and AtT-20 cells, lysates from wild-type (*wt*) and transfected cells expressing either FT-rab 3C (3C) or FT-rab 3D (3D) were probed. The immunodecoration pattern was revealed using an ECL detection system followed by exposure to Hyperfilm. Arrowheads at left indicate the migration of the 29-kD marker (carbonic anhydrase). The relative sizes of FT-rab 3C and FT-rab 3D are 26 and 28 kD, respectively.

To facilitate the detection of rab 3 proteins and to enable distinction between the isoforms, we transfected cells with epitope-tagged rabs 3C and 3D (FT-rab 3C and FT-rab 3D, respectively). Our epitope tag of choice is derived from the influenza virus HA protein and is recognized by the mAb 12CA5. The epitope tag was introduced at the extreme amino terminus of the rab coding sequence; it has previously been shown that such modification does not interfere with rab protein function (Chen et al., 1993). The full-length coding sequence for rab 3D was isolated from rat pituitary (data not shown). Sequence analysis showed that it is highly homologous to the mouse form cloned by Baldini et al. (1992); comparison of the rat and mouse forms revealed only three amino acid differences (of 219 total). We also isolated the coding sequence for rab 3C from AtT-20 cells (data not shown). When compared to the published sequences for rab proteins, this mouse sequence is most homologous to the bovine sequence (Matsui et al., 1988), with 95.4% identity in the predicted amino acid sequence.

We generated several clones of stable transfectants of AtT-20 cells and CHO cells. Immunoblot analysis of cell lysates shows that both FT-rab 3C and FT-rab 3D could be detected with either 12CA5 (anti-HA) or Cl 42.1 (anti-rab 3) (Fig. 6, lanes 3C and 3D), demonstrating that mAb Cl42.1 recognizes both rab 3C and rab 3D. The electrophoretic mobility of FT-rab 3C was slightly greater than that of FT-rab 3D (Fig. 6, compare lanes 3C and 3D). The mAb 12CA5 detected the epitope-tagged proteins only in the transfected AtT-20 and CHO cells; the endogenous rab 3 was not detected by 12CA5, as expected.

To test if the expression of high levels of the epitope-tagged rab 3C and 3D proteins affect the regulated secretory pathway in CHO cells, transfected and wild-type CHO cells were labeled with [^{35}S]sulfate for 30 min, chased for 2 h, and then were incubated in DME (containing 1.8 mM Ca^{2+}) in the absence and presence of A23187 for 10 or 20 min. Wild-type cells secreted 17.56% (SEM = 0.55) and 24.90% (SEM = 0.38) of their stored GAG chains during 10 and 20 min stimulation period, respectively. Cells overexpressing FT-rab 3C secreted 20.00% (SEM = 0.30) and 27.74% (SEM = 0.37), while cells overexpressing FT-rab 3D secreted 19.43% (SEM = 0.48) and 27.49% (SEM = 0.13), respectively (data not shown). Clearly, the overexpression of the FT-rab 3C and -rab 3D constructs in these cells did not impair the function of this pathway, and may even have slightly enhanced the Ca^{2+} -dependent stimulation of GAG chain secretion.

Subcellular Localization of FT-rab 3D Isoforms in AtT-20 Cells

We first examined the subcellular localization of FT-rab 3D in AtT-20 cells, which express and secrete the peptide hormone ACTH via the classical dense-core granule pathway. Transfected and wild-type AtT-20 cells were plated on laminin-treated coverslips and stained by double indirect immunofluorescence with an ACTH-specific polyclonal antibody (1301) and the epitope tag-specific mAb 12CA5 (Fig. 7). In AtT-20 cells, ACTH was primarily distributed in two locations: the process tip and the perinuclear Golgi apparatus (Fig. 7 *a*). The presence of the ACTH precursor, POMC, throughout the early stages of the secretory pathway gives rise to the staining in the Golgi apparatus. Previous studies have demonstrated that the tip staining in AtT-20 cells is localized to dense-core granules (Orci et al., 1987; Tooze et al., 1989). 12CA5 did not stain wild-type AtT-20 cells (Fig. 7 *b*). With AtT-20 cells expressing FT-rab 3D, the ACTH staining pattern was indistinguishable from that pattern seen in wild-type cells (Fig. 7 *c*). The 12CA5 staining pattern closely resembled the ACTH staining pattern, with intense staining at the tips, as well as regions of costaining at points throughout the cell including the extended processes (Fig. 7 *d*). This pattern was specific for the expression of the FT-rab 3D protein, as cells expressing FT-rab 11 exhibited a 12CA5 staining pattern restricted to a juxtannuclear region (arrowheads) while the 1301 pattern was not different from wild-type cells (arrows; Fig. 7, *e* and *f*); no tip staining was detected with 12CA5 in AtT-20 cells that express FT-rab 11. By subcellular fractionation, rab 11 has been associated with the TGN in PC12 cells (Urbé et al., 1993) and with intracellular tubulovesicles in gastric parietal cells (Goldenring et al., 1994). These immunofluorescence data suggest that the FT-rab 3D protein is targeted to regulated secretory pathway in transfected AtT-20 cells.

Indirect Immunofluorescence and Subcellular Fractionation of rab 3D from CHO Cells

We next investigated whether the epitope-tagged rab 3 forms were associated with membranes involved in regulated secretion in CHO cells. Approximately 80% of the

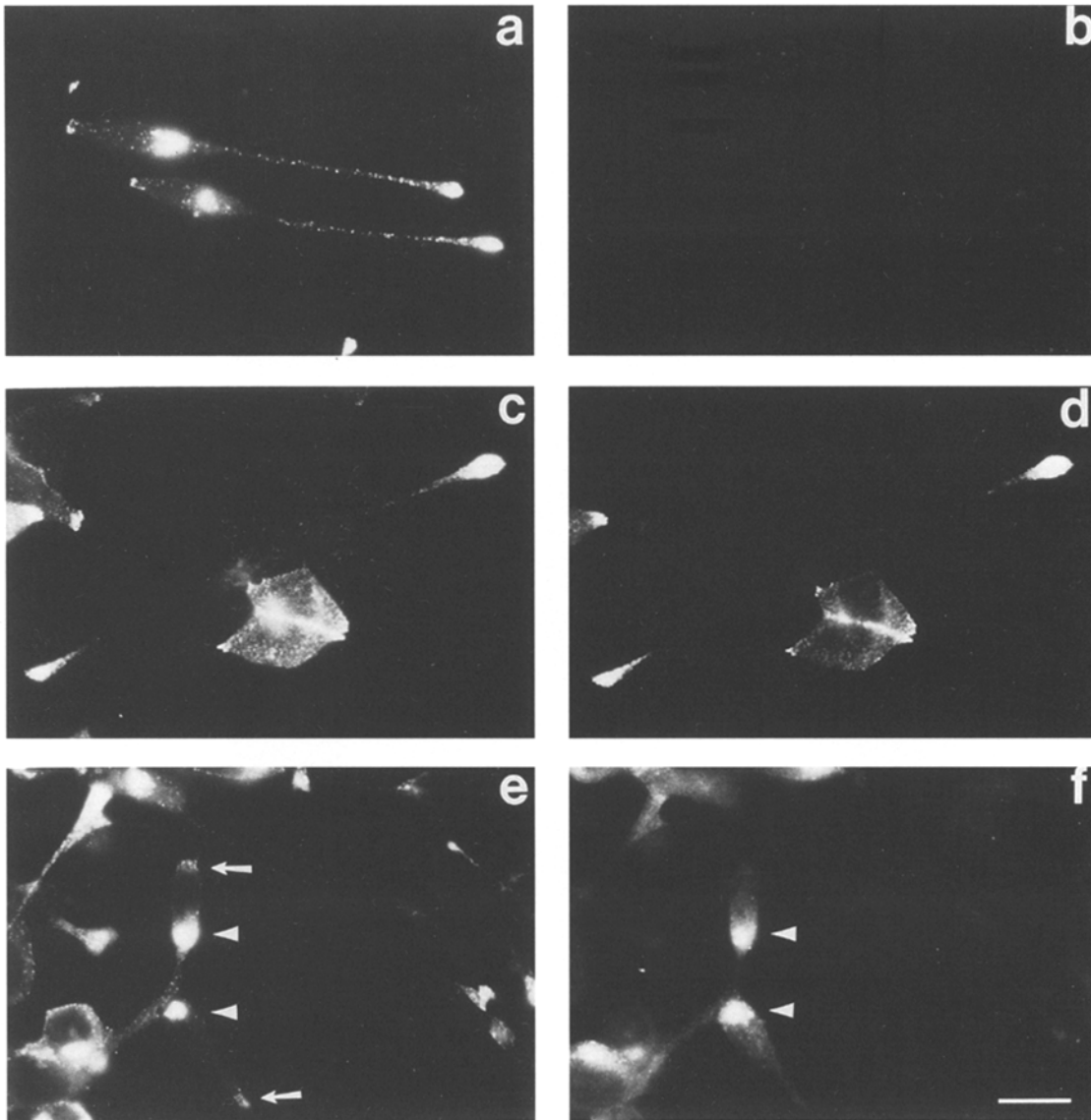


Figure 7. Indirect immunofluorescence localization of ACTH and epitope-tagged rab protein immunoreactivity in wild-type and transfected AtT-20 cells. Wild-type (*a* and *b*) and transfected AtT-20 cells (expressing either FT-rab 3D [*c* and *d*] or FT-rab 11 [*e* and *f*]) were plated on laminin-coated glass coverslips overnight, fixed with formaldehyde, and permeabilized with cold methanol. After blocking with BSA, the cells were costained with the rabbit polyclonal antibody 1301, specific for ACTH (*a*, *c*, and *e*) and the HA epitope-specific mouse mAb 12CA5 (*b*, *d*, and *f*). The second costaining was performed with FITC-conjugated goat anti-mouse IgG antibody and rhodamine-conjugated goat anti-rabbit IgG antibody. In lower panels (*e* and *f*), arrowheads indicate regions stained by 12CA5 and arrows indicate 1301 process tip staining in the same transfected cells. Note that cells expressing FT-rab 11 lack tip staining revealed by 12CA5, but their process tips are stained with 1301. Bar, 20 μ m.

FT-rab 3D in stably transfected CHO cells was membrane-associated and resistant to carbonate extraction (Chavez, R.A., and H.-P.H. Moore, unpublished observations). Indirect immunofluorescence staining of FT-rab 3D-transfected CHO cells yielded reticular staining that was strongest near the nucleus (Fig. 8 *A*). Incubation for 1 h with 0.5 mM xyloside did not alter this staining pattern (data not shown). Martelli et al. (1995) have recently shown that when exogenously expressed in COS cells rab 3D is distributed in a pattern suggestive of the ER. Having seen a similar pattern in our CHO-FT-rab 3D cells, we sought to compare the FT-rab 3D distribution with that of an ER resident protein, calnexin. In CHO-FT-rab 3D cells that were double-labeled with 12CA5 and anti-calnexin,

the calnexin pattern consisted of strong nuclear and nuclear envelope staining, with an even staining pattern in the cytoplasm (Fig. 8 *B*). While the calnexin and FT-rab 3D staining patterns were similar, three differences in the overall patterns could be discerned: the finer and more uniform reticular pattern of calnexin, the strong nuclear envelope staining of calnexin, and the strong perinuclear staining of FT-rab 3D. These data suggest that while FT-rab 3D staining may overlap with the ER (perhaps due to overexpression), the staining pattern for FT-rab 3D is distinct from a solely ER pattern. In addition, it is distinct from the staining pattern of at least one class of recycling endosomes, those containing transferrin receptor (Fig. 8 *C*).

Since GAG chains are sulfated in the TGN, we com-

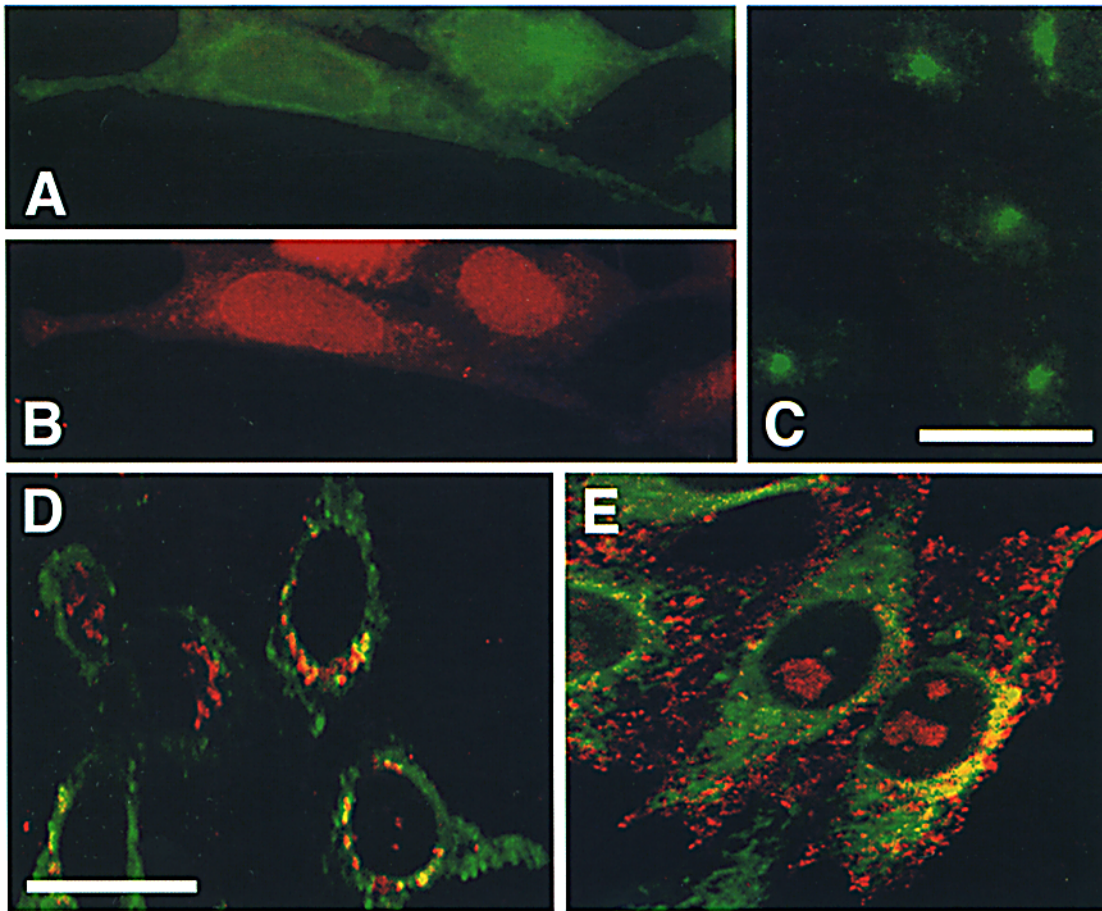


Figure 8. Indirect immunofluorescence localization of FT-rab 3D in transfected CHO cells. CHO cells expressing FT-rab 3D were plated on glass coverslips and processed for immunofluorescence as described above. Primary antibody incubations were followed by FITC-conjugated goat anti-mouse IgG for detection of mAbs (*A–E*), or with rhodamine-conjugated goat anti-rabbit IgG for detection of the polyclonal Ab (*B* and *E*). For *D*, the staining pattern for TGN38-Ig was revealed without a primary antibody but with rhodamine-conjugated goat anti-human IgG for direct detection of the chimeric TGN38-Ig protein. (*A*) Staining with mAb 12CA5 to detect FT-rab 3D. (*B*) Staining with an anti-calnexin polyclonal Ab to detect endogenous calnexin, an ER resident protein. *A* and *B* are of the same cells. (*C*) Staining with mAb H68.4 to detect endogenous transferrin receptor. (*D*) Confocal image (300-nm z-section thickness) of CHO-FT-rab 3D cells transiently transfected with a plasmid encoding the TGN38-Ig chimera. (*E*) Confocal image (300-nm z-section thickness) of CHO-FT-rab 3D cells transiently transfected with a plasmid encoding rat GLUT4. For *D* and *E*, green fluorescence indicates mAb 12CA5 pattern for FT-rab 3D and red fluorescence indicates either the anti-human IgG pattern (*D*) or the anti-GLUT4 pAb pattern (*E*). Yellow fluorescence indicates overlap of staining patterns. *A–C* share the scale bar in *C*; *D–E* share the scale bar in *D*. Bar, 20 μm .

pared the FT-rab 3D distribution in CHO cells with that of an epitope-tagged version of a TGN marker protein, TGN38 (Luzio et al., 1990). Cells expressing both FT-rab 3D (stable) and TGN38-Ig (transient) were analyzed by indirect immunofluorescence (Fig. 8 *D*). While some overlap of the staining pattern was observed, the perinuclear TGN38-Ig staining pattern was distinct from the FT-rab 3D pattern. We also compared the FT-rab 3D distribution in these cells with that of the glucose transporter GLUT4 (James et al., 1989). In PC12 cells GLUT4 has a punctate distribution in the cytoplasm but is segregated away from synaptic-like vesicles containing synaptophysin, and therefore may be localized to a distinct class of recycling-type vesicles. By a velocity gradient analysis GLUT4 was shown to be in vesicles larger in size than PC12 synaptic-like vesicles (Herman et al., 1994) (see below). GLUT4 was expressed in CHO-FT-rab 3D cells by transient trans-

fection, followed by indirect immunofluorescence analysis (Fig. 8 *E*). Confocal microscopy revealed that the staining pattern for GLUT4 in these cells was punctate and showed little overlap with the FT-rab 3D pattern, suggesting that in these cells these two proteins are sorted to distinct intracellular locations. Based on these results, we conclude that overexpression of FT-rab 3D in CHO cells must label either a subcompartment of a known organelle, an entirely novel compartment, or several different organelle types. To characterize further the compartment in which FT-rab 3D resides, we performed subcellular fractionation to determine whether FT-rab 3D was associated with the stored pool of GAG chains in CHO cells.

We sought to resolve the vesicles by relative size using velocity gradient centrifugation. Synaptic vesicles found in PC12 cells were used for comparison for the following reasons. First, synaptic vesicles are low density ($d \sim 1.13$ g/ml;

(Linstedt and Kelly, 1991), similar to that of the GAG-containing membranes in CHO cells. Second, the regulated behavior of the GAG-containing vesicles in CHO cells made it appropriate to compare their physical properties to synaptic-like vesicles from PC12 cells. Synaptic vesicles like those found in PC12 cells are among the smallest regulated secretory vesicles known (50–60 nm).

To compare the synaptic vesicles in PC12 cells and the GAG chain-containing vesicles in CHO cells, FT-rab 3D-transfected CHO cells were first labeled with [³⁵S]sulfate for 30 min and chased in unlabeled medium for 2 h to chase the labeled GAG chains into the post-Golgi storage vesicles. Subcellular fractions were prepared from these cells and from unlabeled PC12 cells and fractionated on a glycerol velocity gradient (Clift-O'Grady et al., 1990). The gradient fractions were pelleted, and assayed for GAG chains by CPC precipitation and for either FT-rab 3D (for the transfected CHO cells) or the synaptic vesicle marker synaptophysin (p38; for PC12 cells) by immunoblotting (Fig. 9). Previous fractionation of synaptic vesicles from PC12 cells have shown that these vesicles, because of their small size, can be recovered in the supernate of a 35-min, 27,000-g spin (S2). When an S2 supernate from PC12 cells was separated on a glycerol velocity gradient spun at 47,000 rpm (264,700 g), synaptophysin immunoreactivity was found in the middle fractions (Chavez, R.A., and H.-P.H. Moore, data not shown), in agreement with previous work (Clift-O'Grady et al., 1990; Linstedt and Kelly, 1991). This slowest-migrating peak containing synaptophysin is defined as synaptic vesicles. In transfected CHO cells, both the stored GAG chains and the FT-rab 3D immunoreactivity were found in the P2 pellet, not the S2 supernate (<5%; Chavez, R.A., and H.-P.H. Moore, data not shown). This result suggested that the labeled GAG chains and FT-rab 3D protein may be found in vesicles larger than synaptic vesicles.

To increase the resolution of larger vesicles in the glycerol gradient, the centrifugation speed was decreased to 25,000 rpm and the postnuclear supernate (S1) from labeled and chased CHO cells was analyzed. When the S1 supernate from transfected CHO cells was spun at 25,000 rpm, the FT-rab 3D protein (as determined by 12CA5 immunodecoration) was predominantly found in fractions 6 to 11 (Fig. 9, middle panel). GAG chain analysis of the same gradient demonstrated that these same fractions contained labeled GAG chains (Fig. 9, bottom panel). The FT-rab 3D-containing vesicles from the S1 supernate detected in this gradient are larger than synaptic vesicles from PC12 cells. After centrifugation at 25,000 rpm, immunoblot analysis of the synaptic vesicle-containing subcellular fraction (S2) from PC12 cells revealed that the synaptophysin immunoreactivity was near the top of the gradient (Fig. 9, top panel, fractions 3–5), indicating that the synaptic vesicles were smaller than the S1 vesicles containing FT-rab 3D and GAG chains. These results suggest that at least a fraction of FT-rab 3D protein in transfected CHO cells cofractionates with GAG chain-containing vesicles, and that these vesicles are larger than synaptic vesicles found in PC12 cells.

As an additional criterion, we separated a postnuclear supernate from [³⁵S]sulfate-labeled CHO-FT-rab 3D cells on a sucrose density gradient. The cells were labeled and

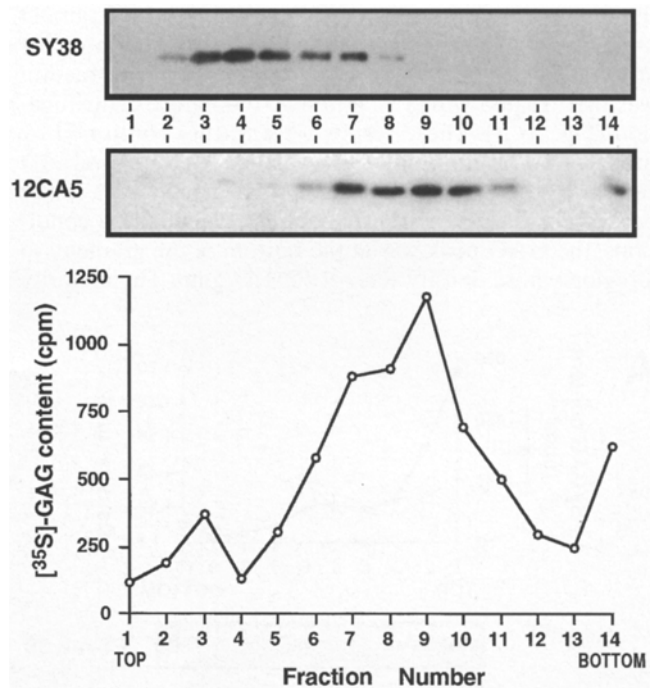


Figure 9. Glycerol velocity gradient analysis of the relative size of the vesicles containing stored GAG chains in FT-rab 3D-expressing CHO cells and synaptophysin-containing vesicles in PC12 cells. An S1 supernate of [³⁵S]sulfate-labeled and -chased CHO cells (expressing FT-rab 3D) and an S2 supernate of unlabeled PC12 cells were prepared as described (see Materials and Methods). The S2 supernate from the PC12 homogenate and the S1 supernate from the CHO cell homogenate were centrifuged through a 5–25% glycerol velocity gradient at 25,000 rpm (74,900 g) for 1 h. The gradients were fractionated and the individual fractions were pelleted. Aliquots from the fractions were analyzed for antigenicity by immunoblot (SY38 for PC12 cells, 12CA5 for transfected CHO cells), and for GAG chain contents. (*Top panel*) Immunoblot of PC12 fractions for synaptophysin. (*Middle and bottom panels*) Fractions from CHO gradient were immunoblotted for FT-rab 3D and assayed for GAG chain content, respectively. The FT-rab 3D peak of immunodecoration detected by 12CA5 represents 11% of the total FT-rab 3D in the S1 supernate; the GAG chain peak represents 27% of the total [³⁵S]sulfate-labeled GAG chains in the S1 supernate. The balance of these materials was lost due either to lysis or to aggregation.

chased as described above. The cells were then homogenized and a postnuclear supernate was separated on a 10–50% sucrose/100% D₂O equilibrium gradient to compare the distribution of GAG chains and the epitope-tagged rab protein (Fig. 10). After fractionation, vesicles from the individual fractions were pelleted at 100,000 g and assayed for GAG chains (by CPC precipitation) and for FT-rab 3D (by immunoblot). The stored GAG chains were found at the top of this gradient (Fig. 10 A, filled circles), indicating that the vesicles in which they are present are not very dense (~1.12 g/ml). The materials found in these fractions are distinct from ER and Golgi membranes, which sediment near the bottom and middle of this gradient, respectively (Miller et al., 1992). The FT-rab 3D protein was found primarily in two peaks, one at the top and the other at the bottom of the gradient (Fig. 10 A, lower panel). The peak of the GAG chains appeared to cofractionate with

the upper peak of the FT-rab 3D profile. The FT-rab 3D immunoreactivity found at the top of the gradient was vesicle associated; this material did not pellet if the fraction was first treated with 1% Triton X-100 before centrifugation (Fig. 10 B). These results were further confirmed by preparing a homogenate from labeled CHO-FT-rab 3D cells and separating it on a similar gradient with a lower percentage of D₂O (50%; Fig. 10 C). Under these conditions, the GAG peak was at the bottom of the gradient, in a region whose density was ~1.12–1.14 g/ml. The majority

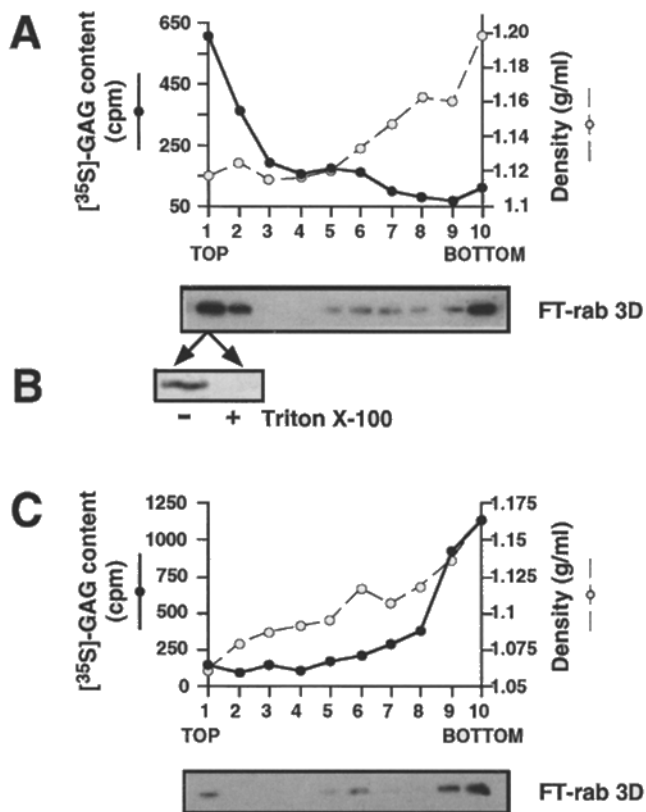


Figure 10. Distribution of stored GAG chains and 12CA5 immunoreactivity from FT-rab 3D-transfected CHO cells fractionated on a D₂O-sucrose equilibrium gradient. (A) GAG content of gradient fractions (10–50% sucrose in 100% D₂O). Transfected CHO cells expressing with FT-rab 3D were labeled with [³⁵S]sulfate and chased as described. The cells were homogenized and separated on a 10–50% (wt/vol) sucrose-D₂O gradient and centrifuged for 3 h at 36,000 rpm (221,600 g) at 4°C. The gradient was fractionated from the top, and membranes from each fraction were pelleted as described. Aliquots of the membrane pellets isolated were assayed for GAG chains (filled circles) as described in Materials and Methods. The density of fractions from a parallel gradient was determined gravimetrically. (B) Immunoblot of D₂O-sucrose gradient fraction #1 (the top of the gradient), with and without Triton X-100 treatment. An aliquot of fraction #1 was split into two portions, solubilized in the absence or presence of 1% Triton X-100 and pelleted at 100,000 g for 40 min at 4°C, and immunoblotted with 12CA5 and analyzed as described. (C) GAG content of gradient fractions (10–50% sucrose in 50% D₂O). Transfected CHO cells expressing with FT-rab 3D were labeled and chased as above. The cells were homogenized and separated on a 10–50% (wt/vol) sucrose-50% D₂O gradient and centrifuged for 3 h at 36,000 rpm at 4°C. Subsequent analysis was identical to that used in A (above).

of FT-rab 3D immunoreactivity was associated with the GAG peak under these conditions. We conclude therefore that a fraction of FT-rab 3D cofractionates with low-density vesicles containing stored GAG chains.

Discussion

To ascertain that a secretory process is regulated, several criteria should be satisfied. The secretory product should be accumulated in an intracellular vesicular compartment. Release of this product should depend on the alteration of the levels of intracellular second messengers. The response to this stimulus should be rapid. We have provided evidence for the presence of a regulated secretory pathway in CHO cells that satisfies each of these criteria. The results described in Fig. 1 demonstrate the accumulation of GAG chains, while the results presented in Figs. 9 and 10 demonstrate the vesicular nature of this storage. The role of only one intracellular messenger, free Ca²⁺ ion, was investigated (Figs. 2–4), but evidence was provided for the possible role of the activation of protein kinase C in the secretion of stored GAG chains from labeled L and CHO cells (Fig. 2). This secretion process occurs within 10 min of incubation with A23187 in the presence of calcium, a time course within the reported range for regulated secretion. Based on this evidence, we conclude that we are observing evidence of a regulated secretory pathway in a constitutive secretory cell line.

Additional evidence suggests that we have observed a regulated pathway which is not a modification of the constitutive pathway. These two pathways can be distinguished by kinetics and by sensitivity to cytoplasmic calcium ion. It seems clear that intact AtT-20, CHO, and L cells have a biphasic secretory pattern. This pattern consists of a fast phase with a short *t*_{1/2} for transport to the cell surface, indicated by the rapid rise in GAG chain release seen in Fig. 1 A (lower panel) and slow phase whose time course is very similar to that of regulated proteins expressed in cells with a regulated secretory pathway (~10 h; Moore and Kelly, 1986). In both intact and semi-intact cells, the kinetics of the fast phase are not altered by secretagogues or changes in Ca²⁺ levels (Miller and Moore, 1991). In contrast, we have demonstrated here that Ca²⁺ has a stimulatory effect on the slow phase (Figs. 1–4).

Why was this regulated pathway not observed before this report? We can propose several factors which may have contributed to our present observations. First of all, we were able to use a single marker to look at both constitutive and regulated secretion in the same labeling protocol. GAG chains, being promiscuous as to sorting, enter both pathways. Protein hormones, on the other hand, may require specific sorting into the regulated pathway. Lacking this, polypeptide hormones may be sorted into the constitutive pathway exclusively and not to the regulated pathway (see below). In addition, the level of constitutive release from radiolabeled constitutive secretory cells is generally too high to detect a regulated signal in response to secretagogues. We surmised however that after the majority of constitutive secretion was completed, it might be possible to observe a regulated signal. Finally, our efforts were aided by the timing of the pulse-chase protocol. Because of the differences in the turnover rates of the two

pathways, a short pulse (5 min) predominantly labels GAG chains in the constitutive pathway; the analysis of any subsequent chase would provide evidence for an efficient constitutive secretory process. As shown in our previous study, following a 2-min pulse, >90% of labeled GAG is secreted with $t_{1/2}$ of 20 min, suggesting that <10% enters the novel pathway after a short pulse (Miller and Moore, 1991, 1992). Increasing the labeling duration would succeed in labeling regulated granules as well, while increased chase times would allow secretion of the constitutive label and decrease the background against which the regulated signal would appear. In this study, our experiments used labeling periods from 30 min to 2 h; hence we arrived at the secretory profile seen in Fig. 1. We were able to detect regulated secretion of GAG chains from CHO and L cells by taking advantage of all of these features in the design of our experiments. Although unlikely, we cannot exclude the possibility that treatment with xyloside has induced this pathway. However, xyloside treatment had no effect on the 12CA5 staining pattern of CHO-FT-rab 3D cells.

The regulated secretory process we have observed is part of the biosynthetic pathway and not the synaptic vesicle-type recycling pathway. GAG chain labeling by [³⁵S]sulfate occurs either in the *trans*-Golgi or in the TGN (Miller and Moore, 1991). We did not observe re-uptake of previously secreted material in CHO cells, as might be expected if recycling of these granules at the plasma membrane did occur. Our velocity gradient analysis of GAG chain-containing granules demonstrates that the GAG chains are contained in structures larger than synaptic vesicles derived from PC12 cells (Fig. 9). It is also very unlikely that we are observing secretion from endosomes or lysosomes. Immunofluorescence staining of FT-rab 3D in CHO cells showed that it did not colocalize with the late endosome marker lgp120 (data not shown), suggesting that GAG chains secreted in response to A23187 did not follow the route taken by the mannose-6-phosphate receptor from the TGN to endosomes. In addition, lysosomes are denser than the GAG-containing organelles and one would not expect that lysosomal contents could be secreted in a regulated fashion.

The GAG chain-containing vesicles in CHO cells are similar to peptide hormone-containing granules in several respects. They have a similar Ca²⁺ dose dependence of secretion (maximal response at 1–5 μM), and both contain rab 3D and turn over slowly in the absence of secretagogues. However, they have several distinct characteristics. Regulated granules from CHO cells are less dense than peptide hormone-containing granules. Mature dense-core granules from PC12 cells have a density of 1.20 g/ml (Linstedt and Kelly, 1991), whereas GAG chains and FT-rab 3D are cofractionated into granules whose density is 1.12 g/ml (Fig. 10, A and C). At present, there is no evidence to suggest that regulated secretory proteins are sorted into the regulated vesicles found in CHO or L cells. When expressed in L cells, regulated proteins like proinsulin are secreted constitutively (Moore et al., 1983a); intracellular storage was not observed even when the labeling period was extended to 16 h, making it unlikely that a storage pool was missed due to short pulse-labeling protocols as discussed above for GAG chains. It is therefore not

clear where the regulated vesicles in CHO cells fall among the *dramatis personae* of regulated secretion. In this regard, it is interesting to note that CHO cells, which lack prohormone endopeptidases, contain carboxypeptidase and amidation activities for producing bioactive peptides (Johansen et al., 1991; Hayashi et al., 1994). With the isolation of a purified population of these vesicles we can investigate their components and determine what similarities they share with other regulated granules.

Recently, Martelli et al. (1995) have described the distribution of endogenously expressed rab 3D in AtT-20 cells. In agreement with their results we found that FT-rab 3D was localized to the process tip in this cell line as well as in punctate structures throughout the cell body (Fig. 7 d). However, they did not compare the distribution of rab 3D with that of the endogenous secretory product ACTH. We found a considerable degree of colocalization of FT-rab 3D and ACTH-containing vesicles especially at the process tip. We would suggest that in AtT-20 cells FT-rab 3D (as well as the endogenous rab 3D) is localized to dense-core granules that contain ACTH. We are currently addressing the nature of the subcellular compartment(s) to which FT-rab 3D is distributed in CHO cells by EM immunocytochemistry.

If the regulated secretory pathway is more widely present than previously thought, then what is the function of this pathway in so-called constitutive cells? This pathway may be involved in intercellular communication in tissues. Autocrine, paracrine, or other chemical signals may either be carried by or be modulators of the regulated pathway in these cell types. One example of this would be the postsynaptic exocytosis observed at the neuromuscular junction by Poo and colleagues (Dan and Poo, 1992). Calcium-dependent secretion from the postsynaptic muscle cell may be involved in synaptic modulation. Muscle cells are good candidates for designation as constitutive cells. A second possible function of this pathway would be analogous to the translocation of plasma membrane proteins such as the insulin-inducible glucose transporter GLUT4 to the cell surface. This pathway is used to insert proteins into the plasma membrane in response to acute needs. It is of interest to note that translocation of GLUT4 to the cell surface can be induced by phorbol esters (Vogt et al., 1991). Recently, Kelly and coworkers have observed that in PC12 cells GLUT4 is targeted to unique vesicles larger than synaptic vesicles, and that these vesicles may be involved in plasma membrane modification (Herman et al., 1994). While our GAG chain- and FT-rab 3D-containing vesicles appear in the same region of the glycerol velocity gradient as GLUT4 vesicles in PC12 cells, our immunofluorescence data lead us to conclude that FT-rab 3D and GLUT4 are targeted to distinct vesicle populations (Fig. 8 E). The regulated transport we have observed is distinct from that seen with surface-expressed membrane proteins such as TGFα and APP. Recent evidence suggests that the release of processed forms of TGFα and APP is caused by the activation of a cell surface protease (Sisodia, 1992; Bosenberg et al., 1993; Arribas and Massagué, 1995). This shedding process is under the regulation of protein kinase C as phorbol esters can stimulate release of both molecules from the appropriate cell lines (Arribas and Massagué, 1995). It appears that the regulated shedding of sur-

face membrane proteins occurs by a different mechanism than the transport process we describe here. However, it is possible that the protease is activated as a result of its transport to the surface by the regulated transport pathway we have observed in constitutive cells. Perhaps like the membrane resealing phenomenon seen in fibroblasts and sea urchin embryos (Steinhardt et al., 1994), this pathway may deal with acute injuries to which all cells may be subjected. The phenomenon we describe could account for some of the vesicles involved in resealing in these cells. Future experiments employing dominant-negative mutants of FT-rab 3D will be important to assess the physiological function of this pathway. Whatever their function is judged to be, it is clear that the vesicles labeled in our assays are involved in biosynthetic protein transport, and as such, constitute the first evidence for regulated biosynthetic transport in so-called constitutive secretory cells.

The authors thank Drs. Louis F. Reichardt and Kathy Buckley for their generous gifts of antibodies, Dr. Richard Fetter for help with the confocal microscopy, and Drs. Frank Bonzelius and Regis B. Kelly for the GLUT4 construct as well as helpful discussions. We thank Ken Teter (Moore laboratory) for the TGN38-Ig construct. The data obtained from the FT-rab 11-expressing AtT-20 cell line (Fig. 7, e-f) was kindly provided by Dr. Y.-T. Chen (Stanford University).

This work was supported by grants from the Public Health Service (GM 35239), the American Cancer Society (CB-89A), and Muscular Dystrophy Association (M1723). R.A. Chavez was supported by a National Science Foundation Minority Postdoctoral Fellowship (BIR 9308057). S.G. Miller was supported by a Merck Fellowship by the Helen Hay Whitney Foundation.

Received for publication 24 March 1995 and in revised form 2 March 1996.

References

- Ahnert-Hilger, F., S. Bhakdi, and M. Gratzl. 1985. Minimal requirements for exocytosis. *J. Biol. Chem.* 260:12730-12734.
- Arribas, J., and J. Massague. 1995. Transforming growth factor- α and β -amyloid precursor protein share a secretory mechanism. *J. Cell Biol.* 128:433-441.
- Baldini, G., T. Hohl, H.Y. Lin, and H.F. Lodish. 1992. Cloning of a Rab3 isotype predominantly expressed in adipocytes. *Proc. Natl. Acad. Sci. USA.* 89:5049-5052.
- Baldini, G., P.E. Scherer, and H.F. Lodish. 1995. Nonneuronal expression of Rab3A: induction during adipogenesis and association with different intracellular membranes than Rab3D. *Proc. Natl. Acad. Sci. USA.* 92:4284-4288.
- Block, M.R., B.S. Glick, C.A. Wilcox, F.T. Wieland, and J.E. Rothman. 1988. Purification of an N-ethylmaleimide sensitive protein (NSF) catalyzing vesicular transport. *Proc. Natl. Acad. Sci. USA.* 85:7852-7856.
- Bosenberg, M.W., A. Pandiella, and J. Massague. 1993. Activated release of membrane-anchored TGF- α in the absence of cytosol. *J. Cell Biol.* 122:95-101.
- Brion, C., S. Miller, and H.-P.H. Moore. 1992. Regulated and constitutive secretion: differential effects of protein synthesis arrest on transport of glycosaminoglycan chains to the two secretory pathways. *J. Biol. Chem.* 267:1477-1483.
- Burgess, T.L., and R.B. Kelly. 1984. Sorting and secretion of adrenocorticotropin in a pituitary tumor cell line after perturbation of the level of a secretory granule-specific proteoglycan. *J. Cell Biol.* 99:2223-2230.
- Burgess, T.L., and R.B. Kelly. 1987. Constitutive and regulated secretion. *Annu. Rev. Cell Biol.* 3:243-293.
- Cardone, M.H., B.L. Smith, W. Song, D. Mochly-Rosen, and K.E. Mostov. 1994. Phorbol myristate acetate-mediated stimulation of transcytosis and apical recycling in MDCK cells. *J. Cell Biol.* 124:717-727.
- Carnell, L., and H.-P.H. Moore. 1994. Transport via the regulated secretory pathway in semi-intact PC12 cells: role of intra-cisternal calcium and pH in the transport and sorting of secretogranin II. *J. Cell Biol.* 127:693-705.
- Chavez, R.A., Y. Chen, W.K. Schmidt, L. Carnell and H.-P.H. Moore. 1994. Expression of exogenous proteins in cells with regulated secretory pathways. *Methods Cell Biol.* 43:263-288.
- Chen, Y.-T., C. Holcomb, and H.-P. Moore. 1993. Expression and localization of two small-molecular weight GTP-binding proteins, rab8 and rab10, by epitope tag. *Proc. Natl. Acad. Sci. USA.* 90:6508-6512.
- Clift-O'Grady, L., A.D. Linstedt, A.W. Lowe, E. Grote, and R.B. Kelly. 1990. Biogenesis of synaptic vesicle-like structures in a pheochromocytoma cell line PC-12. *J. Cell Biol.* 110:1693-1703.
- Dan, Y., and M.-M. Poo. 1992. Quantal transmitter secretion from myocytes loaded with acetylcholine. *Nature (Lond.)* 359:733-736.
- De Camilli, P. 1995. Molecular mechanisms in synaptic vesicle recycling. *FEBS Lett.* 369:3-12.
- Fischer von Mollard, G., B. Stahl, C. Li, T.C. Südhof, and R. Jahn. 1994. Rab proteins in regulated exocytosis. *Trends Biochem. Sci.* 19:164-168.
- Forste, J., D. Hanzel, T. Urushidani, and J. Wolosin. 1989. Pumps and pathways for gastric HCl secretion. *Ann. NY Acad. Sci.* 574:145-158.
- Goldenring, J.R., C.J. Soroka, K.R. Shen, L.H. Tang, W. Rodriguez, H.D. Vaughan, S.A. Stoch, and I.M. Modlin. 1994. Enrichment of rab11, a small GTP-binding protein, in gastric parietal cells. *Am. J. Physiol.* 267:G187-G194.
- Harsay, E., and A. Bretscher. 1995. Parallel secretory pathways to the cell surface in yeast. *J. Cell Biol.* 131:297-310.
- Hayashi, N., T. Kayo, K. Sugano, and T. Takeuchi. 1994. Production of bioactive gastrin from the non-endocrine cell lines CHO and COS-7. *FEBS Lett.* 337:27-32.
- Herman, G.A., F. Bonzelius, A.-M. Cieutat, and R.B. Kelly. 1994. A distinct class of intracellular storage vesicles, identified by expression of the glucose transporter GLUT4. *Proc. Natl. Acad. Sci. USA.* 91:12750-12754.
- James, D.E., M. Strube, and M. Mueckler. 1989. Molecular cloning and characterization of an insulin-regulatable glucose transporter. *Nature (Lond.)* 338:83-87.
- Johansen, T.E., M.M. O'Hare, B.S. Wulff, and T.W. Schwartz. 1991. CHO cells synthesize amidated neuropeptide Y from a C-peptide deleted form of the precursor. *Endocrinology.* 129:553-555.
- Kreiner, T., and H.P. Moore. 1990. Membrane traffic between secretory compartments is differentially affected during mitosis. *Cell Regulation.* 1:415-424.
- Lencer, W., A. Verkman, M.A. Arnaout, and D. Brown. 1990. Endocytic vesicles from renal papilla which retrieve the vasopressin-sensitive water channel do not contain a functional H⁺ ATPase. *J. Cell Biol.* 111:379-389.
- Linstedt, A.D., and R.B. Kelly. 1991. Synaptophysin is sorted from endocytotic markers in neuroendocrine PC12 cells but not transfected fibroblasts. *Neuron.* 7:309-317.
- Luini, A., D. Lewis, S. Guild, D. Corda, and J. Axelrod. 1985. Hormone secretagogues increase cytosolic calcium by increasing cAMP in corticotropin-secreting cells. *Proc. Natl. Acad. Sci. USA.* 82:8034-8038.
- Luzio, J.P., B. Brake, G. Banting, K.E. Howell, P. Braghetta, and K.K. Stanley. 1990. Identification, sequencing and expression of an integral membrane protein of the trans-Golgi network (TGN38). *Biochem. J.* 270:97-102.
- Martelli, A.M., R. Bareggi, G. Baldini, P.E. Scherer, H.F. Lodish, and G. Baldini. 1995. Diffuse vesicular distribution of Rab3D in the polarized neuroendocrine cell line AtT-20. *FEBS Lett.* 368:271-275.
- Martin, T.F.J. 1994. The molecular machinery for fast and slow neurosecretion. *Curr. Opin. Neurobiol.* 4:626-632.
- Matsui, Y., A. Kikuchi, J. Kondo, T. Hishida, Y. Teranishi, and Y. Takai. 1988. Nucleotide and deduced amino acid sequences of a GTP-binding protein family with molecular weights of 25,000 from bovine brain. *J. Biol. Chem.* 263:11071-11074.
- Matteoli, M., K. Takei, R. Cameron, P. Hurlbut, P.A. Johnston, T.C. Südhof, R. Jahn, and P. DeCamilli. 1991. Association of Rab3A with synaptic vesicles at late stages of the secretory pathway. *J. Cell Biol.* 115:625-633.
- Matter, K., and I. Mellman. 1994. Mechanisms of cell polarity: sorting and transport in epithelial cells. *Curr. Opin. Cell Biol.* 6:545-554.
- Miller, S.G., and H.-P.H. Moore. 1990. Regulated secretion. *Curr. Opin. Cell Biol.* 2:642-647.
- Miller, S.G., and H.-P.H. Moore. 1991. Reconstitution of constitutive secretion using semi-intact cells: regulation by GTP but not calcium. *J. Cell Biol.* 112:39-54.
- Miller, S.G., and H.-P.H. Moore. 1992. Movement from the trans-Golgi network to the cell surface in semi-intact cells. *Methods Enzymol.* 219:234-248.
- Miller, S.G., L. Carnell, and H.-P.H. Moore. 1992. Post-Golgi membrane traffic: Brefeldin A inhibits export from the distal Golgi compartment to the cell surface but not recycling. *J. Cell Biol.* 118:267-283.
- Moore, H.-P.H., and R.B. Kelly. 1985. Secretory protein targeting in a pituitary cell line: differential transport of foreign secretory proteins to distinct secretory pathways. *J. Cell Biol.* 101:1773-1781.
- Moore, H.P.H., and R.B. Kelly. 1986. Rerouting of a secretory protein by fusion with human growth hormone sequences. *Nature (Lond.)* 321:443-446.
- Moore, H.-P.H., M. Walker, F. Lee, and R.B. Kelly. 1983a. Expressing a human proinsulin cDNA in a mouse ACTH secretory cell. Intracellular storage, proteolytic processing and secretion on stimulation. *Cell.* 35:531-538.
- Moore, H.P.H., B. Gumbiner, and R.B. Kelly. 1983b. A subclass of proteins and sulfated macromolecules secreted by AtT-20 (mouse pituitary tumor) cells is sorted with adrenocorticotropin into dense secretory granules. *J. Cell Biol.* 97:810-817.
- Oberhauser, A.F., V. Balan, B.C. Fernandez, and J.M. Fernandez. 1994. RT-PCR cloning of Rab3 isoforms expressed in peritoneal mast cells. *FEBS Lett.* 339:171-174.
- Orci, L., M. Ravazzola, M. Amherdt, A. Perrelet, S. Powell, D. Quinn, and H.-P. Moore. 1987. The trans-most cisternae of the Golgi complex: a compartment

- for sorting of secretory and plasma membrane proteins. *Cell*. 51:1039–1051.
- Rothman, J.E. 1994. Mechanisms of intracellular protein transport. *Nature (Lond.)*. 372:55–63.
- Sambrook, J., E.F. Fritsch, and T. Maniatis. 1989. *Molecular Cloning: a Laboratory Manual*. Cold Spring Harbor Laboratory Press, Cold Spring Harbor, New York. 545 pp.
- Saucan, L., and G.E. Palade. 1994. Membrane and secretory proteins are transported from the Golgi complex to the sinusoidal plasmalemma of hepatocytes by distinct vesicular carriers. *J. Cell Biol.* 125:733–741.
- Sculptoreanu, A., E. Rotman, M. Takahashi, T. Scheuer, and W.A. Catterall. 1993. Voltage-dependent potentiation of the activity of cardiac L-type calcium channel α 1 subunits due to phosphorylation by cAMP-dependent protein kinase. *Proc. Natl. Acad. Sci. USA*. 90:10135–10139.
- Sisodia, S.S. 1992. β -Amyloid precursor protein cleavage by a membrane-bound protease. *Proc. Natl. Acad. Sci. USA*. 89:6075–6079.
- Slot, J., H. Geuze, S. Gigengack, G. Lienhard, and D. James. 1991. Immunolocalization of the insulin regulatable glucose transporter in brown adipose tissue of the rat. *J. Cell Biol.* 113:123–135.
- Smith, R., M. Charron, N. Shah, H. Lodish, and L. Jarret. 1991. Immunoelectron microscopic demonstration of insulin-stimulated translocation of glucose transporters to the plasma membrane of isolated rat adipocytes and masking of the carboxyl-terminal epitope of intracellular GLUT4. *Proc. Natl. Acad. Sci. USA*. 88:6893–6897.
- Southern, P.J., and P. Berg. 1982. Transformation of mammalian cells to antibiotic resistance with a bacterial gene under control of the SV40 early region promoter. *J. Mol. App. Genet.* 1:327–341.
- Steinhardt, R.A., G. Bi, and J.M. Alderton. 1994. Cell membrane resealing by a vesicular mechanism similar to neurotransmitter release. *Science (Wash. DC)*. 263:390–393.
- Tooze, J., M. Hollinshead, S.D. Fuller, S.A. Tooze, and W.B. Huttner. 1989. Morphological and biochemical evidence showing neuronal properties in AtT-20 cells and their growth cones. *Eur. J. Cell Biol.* 49:259–273.
- Urbé, S., L.A. Huber, M. Zerial, S.A. Tooze, and R.G. Parton. 1993. Rab11, a small GTPase associated with both constitutive and regulated secretory pathways in PC12 cells. *FEBS Lett.* 334:175–182.
- Vogt, B., J. Mushack, E. Seffer, and H.U. Haring. 1991. The translocation of the glucose transporter sub-types GLUT1 and GLUT4 in isolated fat cells is differently regulated by phorbol esters. *Biochem. J.* 275:597–600.
- White, S., K. Miller, C. Hopkins, and I.S. Trowbridge. 1992. Monoclonal antibodies against defined epitopes of the human transferrin receptor cytoplasmic tail. *Biochim. Biophys. Acta*. 1136:28–34.